PHYSICAL REVIEW A VOLUME 34, NUMBER 2 AUGUST 1986

Pressure broadening of molecular lines in a Stark field

G. Buffa
Gruppo Nazionale Struttura della Materia, Consiglio Nazionale delle Richerche
and Dipartimento di Fisica dell'Università, Piazza Torricelli 2, Pisa, Italy

A. Di Lieto
Scuola Normale Superiore, Piazza dei Cavalieri 7, Pisa, Italy
and Dipartimento di Fisica dell'Università, Piazza Torricelli 2, Pisa, Italy

P. Minguzzi, O. Tarrini, and M. Tonelli
Gruppo Nazionale Struttura della Materia, Consiglio Nazionale delle Ricerche
and Dipartimento di Fisica dell'Università, Piazza Torricelli 2, Pisa, Italy

(Received 13 November 1985)

The collision broadening of Stark-resolved molecular lines is studied both experimentally and theoretically. Accurate measurements are performed on rotational transitions of $^{12}CH_3F$ near 150 GHz and what may be the first experimental evidence of M-dependent pressure broadening of the lines is reported. A simple theoretical model is developed, in the framework of Anderson's theory, to estimate the broadening coefficients of the Stark-resolved components. The theory predicts that the linewidths may depend on M and their average may be different from the zero-field envelope. The calculated values are in good agreement with experimental results, proving that the theoretical approach described in this work is a useful tool to estimate the relevance of the effect in different cases.

I. INTRODUCTION

The problem of collision broadening of spectral lines has been considered by many authors for several decades. Microwave spectroscopy has provided a remarkable amount of data concerning the pressure broadening (PB) of rotational transitions of molecules and several theoretical approaches have been developed to interpret these data in terms of molecular interactions.

However, few of these studies have considered the problems associated with the magnetic degeneracy of the rotational levels in detail. In fact, the presence of a static external field can appreciably affect the PB process and the linewidths of the M components of the transition can be different from each other.[1,2] The most remarkable (and usually ignored) point is that the zero-field width can be quite different from, and usually smaller than, the weighted average of the widths of the various Stark-resolved lines.

The first experimental evidence of such an effect has been obtained in a difficult experiment by Brechignac[3] for an infrared line of methyl fluoride, even if some objection could be raised about the use of different isotopes for the two cases. A deeper study of this phenomenon is desirable because the presence of a Stark field is a very common feature in molecular spectroscopy. Stark modulation is used in many experiments and in some cases a static electric field allows one to bring the line frequencies within the tunability range of the apparatus. These practices are sometimes used even in experiments aimed at PB measurements, but the effect of the field on the line parameters is usually ignored.

The distortion caused by the electric field on the molecular eigenstates cannot account for this effect: Joslin[4] calculated this distortion and predicted a change in the PB coefficient of less than 0.1% for fields up to 10^5 V/cm. The relevant effect of the electric field lies in (partially) removing the M degeneracy: the collisional transitions, that change M within a given J manifold, give a larger contribution to the linewidth when they occur among resolved magnetic sublevels than in the case of degenerate states.

These collision-induced transitions between different sublevels of the same rotational state represent an essentially elastic reorientation of the molecule: the angular-momentum vector is tipped with no change in its magnitude. For some molecules these processes have a significant relevance, as suggested by results on collision-induced transitions in laser-Stark,[5] double-resonance,[6] and time-resolved[7] experiments in infrared spectroscopy.

The importance of measuring the widths of each resolved component has also been pointed out by Schwendeman and Amano[8] in the context of improving the understanding of longitudinal and transversal relaxation times.

Some of the present authors have recently reported about the measurements of the PB coefficients for a few mm-wavelength lines of CH_3Br and CH_3OH.[9] The main feature of the apparatus in Ref. 9 is the ability to measure the width of single resolved M components by a Stark sweep of the lines. In this work we use the same approach, but in a region of higher frequency, and we present a clear evidence of M-dependent linewidths for the case of the $J=3\leftarrow2$, $K=1,2$ rotational transitions of $^{12}CH_3F$.

In Sec. II we describe a theoretical model that, in the frame of impact theory,[10] provides the estimate of the PB coefficients for single resolved components of a symmetric top molecule and their relationship to the degenerate case. In Sec. III the experimental apparatus and the measurement technique are presented while in Sec. IV we discuss the experimental results and the agreement with theoretical predictions.

II. THEORY

Let us consider an isolated molecular line l corresponding to the transition between the initial state $|iJ_i\rangle$ and the final state $|fJ_f\rangle$, induced by the incident electromagnetic radiation. The labels i and f here indicate the set of all quantum numbers other than the angular momentum and its z component. We further assume that the radiation has a fixed polarization ϵ that will be labeled by the jump it can produce in the magnetic quantum numbers, i.e., $\epsilon = M_f - M_i$. In the case of magnetic degeneracy of the rotational states the line l can be considered as the overlap of the lines l_M^ϵ corresponding to the transitions $|f,J_f,M+\epsilon\rangle \leftarrow |iJ_iM\rangle$.

In the presence of an external field, which removes the magnetic degeneracy of the levels, some line components are forced to split. They become completely resolved for a sufficiently large field strength and/or a sufficiently low gas pressure, so that the induced frequency splitting is larger than the broadening of the lines.

For the moment we neglect the effect of Doppler broadening, so each component l_M^ϵ will be described by a Lorentzian profile $F_M^\epsilon(\omega)$ with a width $2\pi n\gamma_M^\epsilon$ and a shift $2\pi n s_M^\epsilon$ from the resonant frequency ω_M^ϵ, which are proportional to the number density n of the gas

$$F_M^\epsilon(\omega) = \frac{C_{MM}^\epsilon}{\pi} \frac{(2\pi n\gamma_M^\epsilon)^2}{(\omega - \omega_M^\epsilon - 2\pi n s_M^\epsilon)^2 + (2\pi n \gamma_M^\epsilon)^2} ,$$

with

$$C_{MM}^\epsilon = \frac{3}{2J_i+1} \langle J_iM \mid 1,\epsilon,J_f,M+\epsilon\rangle^2 .$$

The line-intensity factor C_{MM}^ϵ is normalized to the integrated intensity of the line l, i.e., $\sum C_{MM}^\epsilon = 1$.

Following semiclassical approaches to the impact theory,[10] expressions computable in terms of the intermolecular forces have been already obtained[11–13] for the width and shift coefficients, $\bar{\gamma}$ and $\bar{s}$, of the zero-field line l, described in terms of a single Lorentzian profile.

We can obtain the analogous expression of γ_M^ϵ and s_M^ϵ for the Stark-resolved lines. These line parameters will be computed by means of the complex efficiency function P as follows:

$$\gamma_M^\epsilon + i s_M^\epsilon = \left\langle \int_0^\infty 2\pi b v P_{MM}^\epsilon(b,v,r)\,db \right\rangle_{v,r} . \tag{1}$$

The bracket $\langle\ \rangle_{v,r}$ means thermal average on the relative velocity v of the collision and on the internal energy levels r of the colliding partner. The function $P_{MM}^\epsilon(b,v,r)$ expresses the contribution to the line parameters of a collision with impact parameter b, between the absorbing molecule (a) and a perturbing one (p).

In order to deal with the problem of resolved and nonresolved lines, P is an operator defined in the space of Stark lines $(M,\overline{M})$: the diagonal elements of this operator P_{MM}^ϵ contribute, by Eq. (1), to the single-line parameters, while the off-diagonal elements $P_{M\overline{M}}^\epsilon$ describe interference between neighboring lines. $P_{M\overline{M}}^\epsilon$ can be expressed in terms of the scattering matrix $S = 1 - iT$ describing the internal-state transitions produced in the colliding molecules by the intermolecular potential. In the semiclassical approximation this potential is a time-dependent operator $V_b(t)$ computed along the classical trajectory of impact parameter b and relative initial velocity v:

$$\begin{aligned} P_{M\overline{M}}^\epsilon(b,v,r) = \Big\langle & [\langle iJ_iM,\ rM_r \mid T(b,v) \mid iJ_i\overline{M},\ rM_r\rangle + \langle f,J_f,\overline{M}+\epsilon,\ rM_r \mid T^\dagger(b,v) \mid f,J_f,M+\epsilon,\ rM_r\rangle]^2 \delta_{M\overline{M}} \\ & -2 {\sum}' \langle iJ_iM,\ rM_r \mid T(b,v) \mid iJ_i\overline{M},\ r'M_r'\rangle \langle f,J_f,\overline{M}+\epsilon,\ r'M_r' \mid T^\dagger(b,v) \mid f,J_f,M+\epsilon,\ rM_r\rangle \Big\rangle_{\text{av}} , \end{aligned} \tag{2}$$

where ${\sum}'$ stands for the sum over all primed indices and $\langle\ \rangle_{\text{av}}$ for the average on the magnetic quantum number M_r of the perturbing molecule.

By inspection of the terms contributing to $P_{M\overline{M}}^\epsilon(b,v,r)$ in the right-hand side of Eq. (2), it appears that the first two "outer" terms are diagonal in M, and moreover they are M independent because of rotational symmetry considerations. So they give identical contributions to each Stark component. Therefore the only term which exhibits an M dependence is the third subtractive "middle" term, bilinear in T. This term is also the only one expressing interference between different Stark lines. It follows that, when the "middle" term is null, then all the splitted components have the same width and shift and do not interfere with each other by collisions.

Since an exact calculation of the matrix T is not easily performed, Anderson[14] proposed to distinguish the collisions into two classes: "strong" and "weak."

For the strong case every correlation is lost during the collision, so that

$$P_{M\overline{M}}^{\epsilon,\text{strong}}(b,v,r) = \delta_{M\overline{M}} .$$

For weak collisions P^{weak} is obtained by a perturbative expansion of T, at the lowest order in the intermolecular potential V.

For intermediate b values various approximations are possible and can be found in the literature.[11–16] Some of them introduce corrections for the curvature of the trajectory and for higher-order perturbative terms. However, in the case of molecules with large dipole moment (as for CH_3F) all these approaches produce small differences in the computed results. Therefore we follow the most practical and commonly used approximation which consists of defining a cutoff radius b_0. For $b > b_0$ one assumes $P = P^{\text{weak}}$ while for $b < b_0$ $P = P^{\text{strong}}$. b_0 itself is defined by imposing the unitary upper bound to P^{weak}, i.e.,

$$|P_{MM}^{\epsilon,\text{weak}}(b_0,v,r)|=1\ ; \tag{3}$$

note that both the real and the imaginary part of P^{weak} are taken into account to determine b_0. Thus for a given interaction V between molecules one can calculate the line parameters γ_M^ϵ and s_M^ϵ for the Stark components and compare them to the parameters $\bar{\gamma}$ and $\bar{s}$ of the unsplitted line given by

$$\bar{\gamma}+i\bar{s}=\left\langle \int_0^\infty 2\pi b v \bar{P}(b,v,r)db \right\rangle_{v,r} ,$$

where[17]

$$\bar{P}(b,v,r)=\sum_{M,\bar{M}} I_M^\epsilon P_{M\bar{M}}^\epsilon(b,v,r) I_{\bar{M}}^\epsilon$$

and

$$I_M^\epsilon=\left[\frac{3}{2J_i+1}\right]^{1/2}\langle J_i M\mid 1,\epsilon,J_f,M+\epsilon\rangle$$

is the amplitude of the Stark component l_M^ϵ. These expressions lead to the interpretation of the efficiency function $\bar{P}$ as the zeroth-order term of the expansion in moments of the $P_{M\bar{M}}^\epsilon$ operator in the space of Stark lines.

The following remarks may be useful to clarify the relationship between $\bar{P}$ and P_{MM}^ϵ. Each outer term in Eq. (2), being M independent as stated above, gives equal contributions to both efficiency functions; therefore the difference between $\bar{P}$ and P_{MM}^ϵ comes only from the "middle" terms. Such a difference is essentially due to the presence of reorientational transitions. In fact only (collision-induced) transitions with $\Delta J=0$ and $\Delta M=0$ contribute to the middle term of P_{MM}^ϵ, while all transitions with $\Delta J=0$, both with $\Delta M=0$ and with $\Delta M\neq 0$, contribute to $\bar{P}$. In general the middle terms are subtractive, with the result that in the presence of reorientational transitions the width $\bar{\gamma}$ is expected to be smaller than the width γ_M^ϵ. The magnitude of this reduction is related to the importance of reorientational transitions.

At this point we give the explicit calculations of self-broadening for the case of a gas of symmetric top molecules, interacting with a potential which is dominated by dipole-dipole forces. If we label with J,K,M and J_r,K_r,M_r the rotational states of the absorber and the perturber, respectively, Eq. (1) becomes

$$\gamma_M^\epsilon+is_M^\epsilon=\left\langle \pi v b_0^2+2\pi v\int_{b_0}^\infty b P_{MM}^{\epsilon,\text{weak}}db \right\rangle_{v,J_r,K_r} , \tag{4}$$

where the cutoff radius depends on ϵ,M,v,J_r,K_r according to Eq. (3). Assuming a classical straight-line path in the collision one obtains

$$\begin{aligned}
P_{M\bar{M}}^{\epsilon,\text{weak}}(b,v,J_r,K_r)=\sum_{J_r'}\frac{c_{dd}}{b^4}\,|\langle J_r'K_r\mid 10J_rK_r\rangle|^2
&\times\left\{\sum_{J'}|\langle J'K\mid 10J_iK\rangle|^2\left[f_{dd}\left[\frac{\omega_i+\omega_p}{v}b\right]+i\phi_{dd}\left[\frac{\omega_i+\omega_p}{v}b\right]\right]\delta_{M\bar{M}}\right.\\
&+\sum_{J'}|\langle J'K\mid 10J_fK\rangle|^2\left[f_{dd}\left[\frac{\omega_f+\omega_p}{v}b\right]-i\phi_{dd}\left[\frac{\omega_f+\omega_p}{v}b\right]\right]\delta_{M\bar{M}}\\
&\left.-2\langle J_iK\mid 10J_iK\rangle\langle J_fK\mid 10J_fK\rangle f_{dd}\left[\frac{\omega_p}{v}b\right]R_{M\bar{M}}^\epsilon\right\} ,
\end{aligned} \tag{5}$$

where $\hbar\omega_i=E_i^{(a)}-E_{i'}^{(a)}$, $\hbar\omega_f=E_f^{(a)}-E_{f'}^{(a)}$, $\hbar\omega_p=E_r^{(p)}-E_{r'}^{(p)}$ are the energy jumps involved in the collision

$$c_{dd}=\frac{4\mu^4}{9v^2\hbar^2} ,$$

and Eq. (4) can be written as

$$\gamma_M^\epsilon+is_M^\epsilon=\langle \pi v b_0^2[1+\sigma_{MM}^{\epsilon,\text{weak}}(b_0,v,J_r,K_r)]\rangle_{v,J_r,K_r} . \tag{6}$$

The expression for $\sigma_{MM}^{\epsilon,\text{weak}}$ in Eq. (6) is the same as Eq. (5) for $P_{MM}^{\epsilon,\text{weak}}$, except that the functions f_{dd} and ϕ_{dd} are replaced by F_{dd} and Φ_{dd}. The functions f_{dd}, ϕ_{dd}, F_{dd}, and Φ_{dd} can be found in the literature.[11,12,18,19] The M dependence is expressed in Eqs. (5) and (6) by the factor

$$R_{M\bar{M}}^\epsilon=\langle J_iM\mid 1,M-\bar{M},J_i,\bar{M}\rangle \times\langle J_f,\bar{M}+\epsilon\mid 1,M-\bar{M},J_f,M+\epsilon\rangle .$$

For $M=\bar{M}$ one has

$$R_{MM}^\epsilon=\frac{M}{[J_i(J_i+1)]^{1/2}}\frac{M+\epsilon}{[J_f(J_f+1)]^{1/2}} ; \tag{7}$$

note that the corresponding factor $\bar{R}$ in the middle term for the unsplit linewidth $\bar{\gamma}$ is

$$\begin{aligned}\bar{R}&=\tfrac{1}{3}\sum_{M,\bar{M},\epsilon}\langle J_iM\mid 1,\epsilon,J_f,M+\epsilon\rangle\\&\quad\times R^{\epsilon}_{M\bar{M}}\langle J_i\bar{M}\mid 1,\epsilon,J_f,\bar{M}+\epsilon\rangle\\&=(-1)^{J_i+J_f}[(2J_i+1)(2J_f+1)]^{1/2}W(J_iJ_iJ_fJ_f;11)\\&=\frac{J_i(J_i+1)+J_f(J_f+1)-2}{2[J_i(J_i+1)J_f(J_f+1)]^{1/2}}\;. \qquad (8)\end{aligned}$$

On comparing Eqs. (7) and (8) it can be seen that $\bar{R}$ is larger than R^{ϵ}_{MM} and this is particularly remarkable for low M values. The subtractive middle term is smaller (and the width larger) for the Stark-split lines than for the degenerate case at zero field.

III. EXPERIMENTAL

In the design of the experimental apparatus we tried to solve one of the main difficulties of conventional spectrometers: the troublesome effect of standing waves. In fact, in a waveguide cell the power reaching the crystal detector strongly depends on the radiation frequency, because of unwanted reflections within the microwave circuit. A good matching at any given frequency can be obtained by properly adjusting the waveguide components, but it is difficult to maintain this matching under swept-frequency conditions. The consequent distortions in the observed line shape spoil the measurement accuracy and the problem is more and more difficult as the frequency is increased into the mm-wavelength region. Thus in this region the PB measurements are essentially fixed-frequency experiments and one is led to borrow the method of Stark-sweep measurement from infrared laser-Stark spectroscopy. In this approach the frequency of the source is kept fixed and the different Stark components of the line are tuned into resonance by sweeping the electric field. Of course, this method allows only the measurement of PB for each resolved component and in this sense it yields information complementary to that obtained by conventional spectrometers.

The experimental apparatus is illustrated by the block diagram in Fig. 1. Its main structure is similar to that described in Ref. 9 but some improvements have been made and a few details are different. The absorption cell is a hybrid Fabry-Perot interferometer of the type first described in Ref. 20. It consists of a hemifocal resonator with a flat and a cylindrical mirror enclosed between two conducting plates. The plates are 84 cm long and 20 cm wide with a nominal distance of 16 mm; the cylindrical mirror has a radius of curvature of 5 m and the resonator Q is about 5×10^4 at frequencies near 150 GHz. The whole structure (mirrors and plates) is supported by a rugged superinvar frame, to ensure a good thermal and mechanical stability. The interferometer is contained in a chamber connected to a conventional vacuum system, consisting of a diffusion and a rotary pump.

During the measurements the chamber is filled with the desired amount of the sample gas and it is sealed by a high-vacuum valve. The gas pressure is measured by a capacitance manometer with a resolution of 0.01 Pa and an estimated accuracy of 0.1 Pa. The stated purity of the CH_3F sample (Matheson Corp.) is 99.0%, in natural abundance of isotopic species; all measurements are taken at room temperature (298—300 K).

The radiation source is an E-band klystron phase locked to a high-spectral-purity quartz oscillator. The phase-lock loop contains an additional mixer that allows computer control of the klystron frequency via a programmable radio-frequency synthesizer. The spectrum of the beat signal at the input of the klystron synchronizer is shown in Fig. 2. The high signal-to-noise ratio allows a very accurate operation of the stabilization loop. The short-term frequency stability for the overall system is

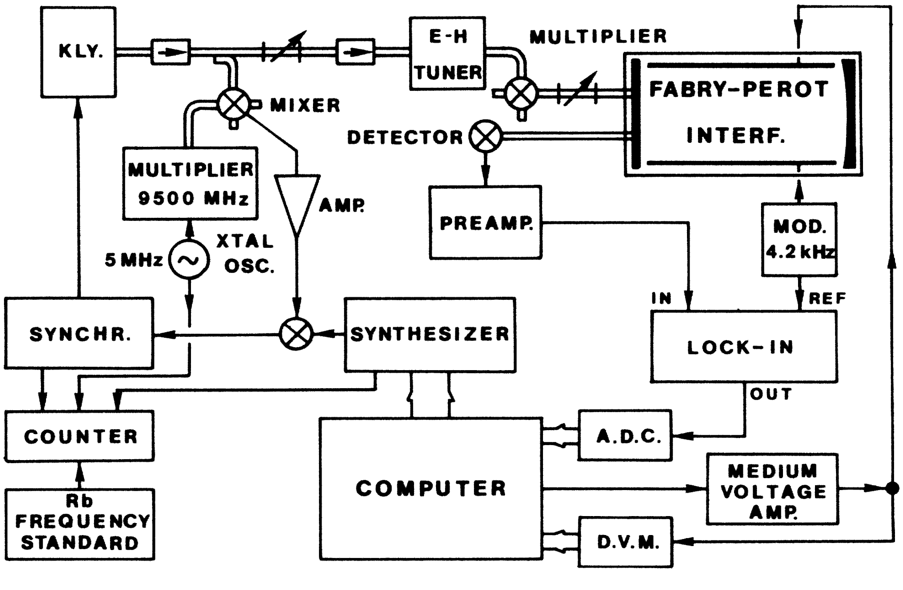

FIG. 1. Schematic diagram of the experimental apparatus used for linewidth measurement in the mm-wavelength region.

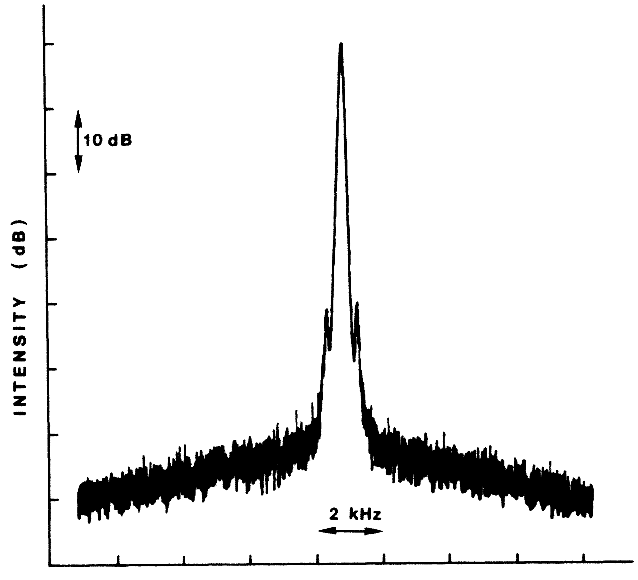

FIG. 2. Spectrum analyzer recording of the feedback signal at the input of the synchronizer under closed-loop conditions. The vertical scale is logarithmic and the center frequency is 40 MHz. The analyzer conditions are bandwidth 100 Hz, video filter 10 Hz, scan time 10 sec/div.

better than 10^{-9}. The radiation frequency is doubled in a crystal harmonic generator (a W-Si diode from Custom Microwave); the matching can be optimized by means of a phase shifter and an E-H tuner placed in the E-band section of the circuit. The harmonic energy from the high-frequency port of the multiplier is directly sent, after attenuation, to the Fabry-Perot resonator. The transmitted power is detected by a GaAs Schottky-barrier diode coupled to a low-noise preamplifier and a bias circuit.

To measure the absorption line shape a voltage ramp is applied to the plates with a superimposed 4.2-kHz modulation voltage. The whole data-acquisition sequence is managed by a microcomputer. The voltage sweep is generated by a digital-to-analog converter with 16-bit resolution, driving a low-noise medium-voltage amplifier. At each ramp step the actual voltage on the plates is directly read by a digital voltmeter with a resolution of $5\frac{1}{2}$ digits. The estimated accuracy of the voltage measurements is 0.01%. The absorption signal from the detector is processed by a lock-in amplifier tuned to the frequency of Stark modulation, so derivative line shapes are observed. The lock-in output is digitized by a 12-bit analog-to-digital converter, and a forward and a backward ramp are averaged to avoid systematic effects. Each measurement run generates a data set consisting of (voltage, signal) pairs which are stored, displayed, and on-line fitted with the derivative of a Lorentzian line shape.

The linewidth so obtained is expressed in "voltage" units and can be converted to frequency units by using the frequency-to-voltage relation of each resolved line component. An expression of sufficient accuracy is

$$\nu_M(\mathscr{V}) = \nu_0 + \alpha_M \mathscr{V} + \beta_M \mathscr{V}^2 , \tag{9}$$

where ν_M is the frequency of the M component at the applied voltage $\mathscr{V}$, ν_0 is the unperturbed frequency, and the parameters α_M and β_M are complicated functions of the dipole moment and the transition quantum numbers, but also of the plate distance d and voltmeter nonlinearity. They are best determined by a direct experimental calibration as explained in the following.

We studied the rotational transitions $J = 3 \leftarrow 2$, $K = 1$, and $K = 2$ in the ground vibrational state of $^{12}CH_3F$ near 153 GHz. The mm-wavelength radiation is orthogonally polarized to the static electric field, thus only $\Delta M = \pm 1$ transitions are allowed. The effect of a Stark field $\mathscr{E} = \mathscr{V}/d$ on the rotational levels of methyl fluoride is easily calculated,[21] and the corresponding shift in the line frequency can be written as

$$\nu_M(\mathscr{E}) = \nu_0 + \Delta\nu_1 + \Delta\nu_2 + \cdots ,$$

where $\Delta\nu_1$ and $\Delta\nu_2$ are the first- and second-order perturbation terms, respectively.

The explicit expression of $\Delta\nu_1$ for the case of the transitions $(J = 3, K, M \pm 1) \leftarrow (J = 2, K, M)$ is

$$\Delta\nu_1(\mathscr{E}) = \frac{\mu\mathscr{E}}{h} \frac{K(M \mp 1)}{12} , \quad -2 \le M \le 2 .$$

So for each $K \neq 0$, there are ten components: among these, two have a null first-order Stark shift and four are (in pairs) different only for the second-order terms. Since in our operating region of fields and pressures $\Delta\nu_2$ is smaller than the width of single lines, we could measure the broadening of only four well-resolved transitions for each K value.

A set of preliminary measurements was taken to estimate the resonant field of each component for many different values of the source frequency. These data allowed us to compute the coefficients α_M and β_M of Eq. (9). To improve the accuracy we used also the results of measurements, performed at low pressure and high power, featuring a narrow Lamb dip at the center of Doppler profile.[22] Note that the use of the relation (9) for each component bypasses the problem of an absolute calibration of the electric field strength.

Other possible pitfalls, such as saturation or modulation additional broadening, have been tested by measuring the apparent linewidth as a function of the incident power and of the modulation amplitude (see also Ref. 9). The sensitivity of the spectrometer is sufficiently high to allow measurements in conditions where these effects are well below 1% of the linewidth.

After these preliminary checks, several runs have been taken for each component. Results have been collected in the pressure range between 0.6 and 3.5 Pa, and for different settings of the source frequency, up to a maximum detuning of 50 MHz. The applied fields are in the range 0–180 V/cm.

IV. RESULTS AND DISCUSSION

In Fig. 3 we show an example of a spectrum obtained by a wide scan of the Stark voltage. This kind of prelimi-

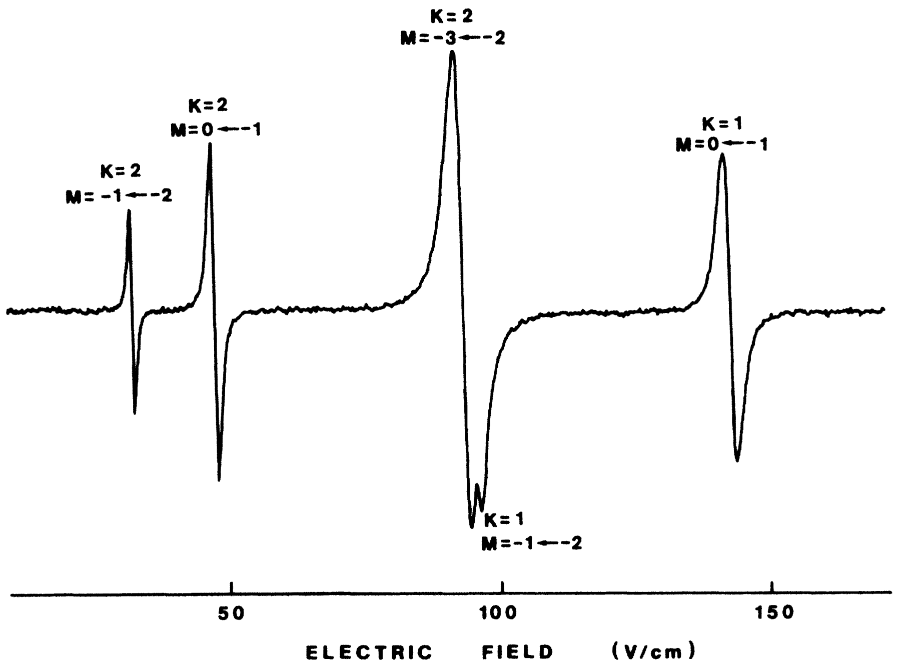

FIG. 3. Survey Stark spectrum of the $J=3\leftarrow2$ rotational line of $^{12}CH_3F$ at a source frequency of 153 185 296.4 kHz.

nary recording is usually taken to check whether the selected component is well isolated from the neighboring lines. In fact, it can be noted that accidental coincidences of $K=1$ and $K=2$ components may sometimes happen at a given setting of the source frequency. In such cases the frequency is changed to a different value and only measurements on well-resolved lines are used to evaluate the PB coefficient. A much narrower scan is used to study single lines: typically 100 samples are taken spanning about four linewidths on both sides of the line center.

Occasionally we tried to measure the broadening of some blended lines which have an appreciably stronger intensity than the others. These measurements warned us about the importance of the corrections which are necessary when the absorption path length becomes comparable to the inverse of the peak absorption coefficient (see, e.g., Ref. 23). For the cases of the fully resolved components studied in this work, this correction ranges from 0.5% to 5%.

The rough experimental data obtained from the line-shape fitting are converted to frequency units by using the appropriate coefficients in Eq. (9) and the correction for the path length is applied according to Eq. (2) of Ref. 23. The results concerning four of the eight fully resolved components are shown in Fig. 4. It can be clearly noted that the pressure dependence of the observed widths is not perfectly linear: this is essentially a consequence of the Doppler effect. In fact, in the pressure range we investigated, the contribution of Doppler broadening to the line shapes is not negligible, so actually a Voigt profile is a better line-shape model than a simple Lorentzian curve. However, a simple method can be used to deal with this problem:[24] this method is based on a rational expansion for the width of a Voigt profile in terms of the collisional and Doppler contributions. The continuous curves in Fig.

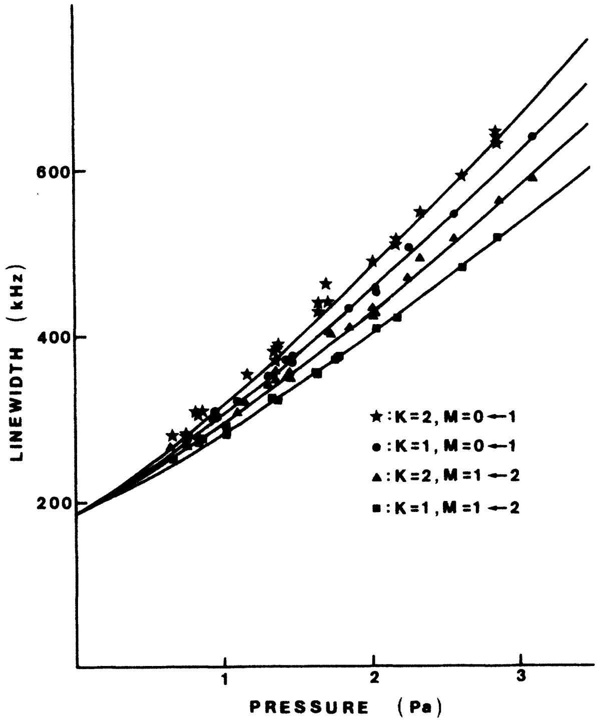

FIG. 4. Collisional linewidth (half width at half maximum) as a function of pressure for four well-resolved Stark components. The experimental data for the other four symmetrical lines are practically coincident with those presented here and have been omitted for clarity. The continuous curves are the best fits to the data, as explained in the text, and they all tend to the Doppler width.

4 are the best fits of this expansion to each data set; an important feature is that the values extrapolated to zero pressure are all coincident with the theoretical Doppler width of the lines (within the experimental error).

The PB coefficients obtained by this fitting procedure are reported in Table I together with their estimated accuracy. A first inspection of these results shows that the line components which are symmetrical in the M pattern display an almost coincident broadening. Of course, this is also expected by parity considerations, so we also report the coefficients obtained by a simultaneous fit of the model curve to all of the data available for each symmetrical pair of lines.

The accuracies quoted in Table I for our experimental results stem from four main sources of error which are discussed in order of importance. The statistical fluctuations in the measurements give a contribution to error ranging from 0.7% to 2% (at 95% confidence level). Residual effects of power broadening are usually important at low pressures and, from the width values extrapolated to zero pressure, we estimate that their contribution is typically 0.5%. A contribution to the error of about the same amount comes from the effect of inhomogeneity in the static electric field. This has been estimated from control measurements taken at fields above 1.5 kV/cm and scaling it to our operating range. Residual modulation broadening has been checked as described in Sec. III and no significant effect has been found; by use of Eq. (12) of Ref. 24 we estimate its contribution to the error to be about 0.2%.

The errors quoted in Table I do not take into account the possible absolute inaccuracy derived from the calibration of the capacitance manometer. This calibration does not affect the relative values of PB coefficients, so we did not include it into the error estimates of Table I to remark the significancy of the differences observed between the Stark components. If the calibration error is brought in, we conservatively estimate that the overall accuracy of the broadening coefficients reported in this work is about 3%.

The theoretical results reported in Table I have been computed by means of Eqs. (5)–(8) for a temperature of 300 K and using the well-known molecular constants of $^{12}CH_3F$. The following points are worth noting:

(i) the zero-field widths of $K=1$ and $K=2$ lines are different;

(ii) the widths of the Stark-resolved components are larger than those of the unsplit lines, as expected;

(iii) the resolved $K=1$ components are narrower than the corresponding ones with $K=2$, just the opposite of the zero-field case;

(iv) symmetrical lines have the same PB coefficient: in the computation the additional Stark energy is negligible in comparison to the rotational splitting.

In view of the approximations involved in the theory, the calculated results have an estimated absolute accuracy of the order of 10%.

The experimental results are in good agreement with calculated values and, remarkably, they follow the expected features (iii) and (iv) discussed above. The trend with M is also respected; however, the observed M dependence is larger than that predicted by the theory, particularly for the $K=1$ lines. This may be ascribed to the theoretical approximations, however, since the $K=1$, $M=0\leftarrow\pm1$ lines are the most intense we studied, we cannot exclude that the path-length correction is not fully adequate for them.

For comparison we report in Table I also the results of Birnbaum *et al.*[25] for unsplit lines obtained with a conventional spectrometer. They quote the measurement accuracy only for the $K=2$ line and they report that they did not observe a significant difference in the broadening of different K lines. However, as remarked in Sec. III,

TABLE I. Pressure-broadening coefficients (kHz/Pa, half width at half maximum) for the $J=3\leftarrow2$ rotational line of $^{12}CH_3F$ and its Stark components. Results for both single and simultaneous fits of symmetrical pairs of lines are reported. As explained in the text the results in the last column are normalized to the experimental value of the $K=2$, $M=0\leftarrow\pm1$ width.

Line	Calc.	Measured Single	Measured Pair	Calc.[b]
$K=2$, $M=-1\leftarrow-2$	186.0	175.4 (2.3)	174.0 (2.4)	178.8
$K=2$, $M=1\leftarrow2$	186.0	171.1 (2.9)		
$K=2$, $M=0\leftarrow-1$	200.3	201.0 (2.7)	201.2 (2.6)	201.2
$K=2$, $M=0\leftarrow1$	200.3	201.7 (3.2)		
$K=2$ unresolved	133.5	129.0 (4.5)[a]		111.8
$K=1$, $M=-1\leftarrow-2$	166.5	148.6 (3.0)	151.7 (2.4)	195.6
$K=1$, $M=1\leftarrow2$	166.5	153.7 (2.4)		
$K=1$, $M=0\leftarrow-1$	171.0	176.1 (2.5)	176.5 (2.4)	201.2
$K=1$, $M=0\leftarrow1$	171.0	177.0 (2.8)		
$K=1$ unresolved	153.0	129.0[a]		178.8

[a] Reference 25.

[b] Computed from Eqs. (1)–(3) of Ref. 3.

this was a difficult measurement for a conventional apparatus, so the results of Ref. 25 cannot be considered as a definitive disproof of the prediction (i). A last comparison between our experimental results and those of Ref. 25 seems to support also the expected feature (ii), i.e., narrower lines for the unsplit case, even if some caution should be exercised in comparing PB results obtained in different laboratories with different spectrometers.

In the last column of Table I we compare our results with the predictions of the theoretical approach proposed in Ref. 3. The latter approach is appealing since it allows one to express the width as the product of a constant quantity, $Q^s(1,0,0)$, and a geometrical factor, depending on the quantum numbers of the transition. Thus one can directly determine the ratios of the various linewidths. We used Eqs. (1) and (3) of Ref. 3 to compute these ratios and we normalized the data in the last column of Table I to the measured width of the $K=2$, $M=0\leftarrow\pm1$ line, which appears one of the most reliable experimental results. The resulting M dependence of the linewidth is slightly larger than ours, but not very different. On the contrary the predicted K dependence is definitely different and leads to two conclusions which are contradicted by our measurements: (i) the $M=0\leftarrow\pm1$ widths should not depend on K, (ii) the $M=\pm1\leftarrow\pm2$ widths should be larger for $K=1$ than for $K=2$. The origin of such discrepancies can be understood by observing that the same results could be derived from our Eqs. (5)–(8) by neglecting the strong part of $P(b,v,r)$ and by assuming that the energy jumps ω_i, ω_f, and ω_p of Eq. (5) are much smaller than v/b, the inverse of the collision time. Such an approximation appears rather rough for the lines studied here, since $\omega b/v$ is of the order of unity.

In conclusion it may be stated that in this work we report what may be the first experimental evidence of different collision broadening for the resolved Stark components of a molecular line. This achievement has been possible by a careful design of the experimental apparatus, allowing accurate measurements in the frequency region beyond 100 GHz. A simple theoretical approach has been presented, which is a straightforward generalization of the old Anderson's impact theory; this model allows the computation of the absolute values of PB coefficients for the resolved components and their comparison with the unsplit case. All the theoretical predictions are confirmed by our experiment and also the agreement in absolute results is very satisfactory. The importance of the effect described here is related to the magnitude of elastic reorientation cross sections, so it can be more pronounced for some molecules than for others. However, the theoretical approach of Sec. II appears a useful tool to estimate its relevance in different cases.

ACKNOWLEDGMENTS

This work has been partially supported by Gruppo Nazionale Struttura della Materia del Consiglio Nazionale delle Ricerche and by Ministero della Pubblica Istruzione.

---

[1] A. Di Giacomo, Nuovo Cimento **44B**, 140 (1966).
[2] H. M. Pickett, J. Chem. Phys. **61**, 1923 (1974).
[3] Ph. Brechignac, J. Chem. Phys. **76**, 3389 (1982).
[4] C. J. Joslin, Mol. Phys. **47**, 677 (1982).
[5] J. W. C. Johns, A. R. W. McKellar, T. Oka, and M. Roemheld, J. Chem. Phys. **62**, 1488 (1975).
[6] R. L. Shoemaker, S. Stenholm, and R. G. Brewer, Phys. Rev. A **10**, 2037 (1974).
[7] Ph. Brechignac, A. Picard-Bersellini, and R. Charneau, J. Phys. B **13**, 135 (1980).
[8] R. H. Schwendeman and T. Amano, J. Chem. Phys. **70**, 962 (1979).
[9] P. Minguzzi, G. Carrara, M. Tonelli, and A. Di Lieto, J. Mol. Spectrosc. **109**, 395 (1985).
[10] M. Baranger, Phys. Rev. **111**, 481 (1958).
[11] C. J. Tsao and B. Curnutte, J. Quant. Spectrosc. Radiat. Transfer **2**, 41 (1962).
[12] B. S. Frost, J. Phys. B **9**, 1001 (1976).
[13] D. Robert and J. Bonamy, J. Phys. (Paris) **40**, 923 (1979).
[14] P. W. Anderson, Phys. Rev. **76**, 647 (1949).
[15] J. S. Murphy and J. E. Boggs, J. Chem. Phys. **47**, 691 (1967).
[16] R. P. Leavitt and D. Korff, J. Chem. Phys. **74**, 2180 (1981).
[17] G. Buffa and O. Tarrini, Phys. Rev. A **16**, 1612 (1977).
[18] C. Boulet, D. Robert, and L. Galatry, J. Chem. Phys. **65**, 5302 (1976).
[19] J. K. Messer, B. Khoobehi, and J. A. Roberts, J. Chem. Phys. **76**, 2914 (1982).
[20] J. Legrand, B. Segard, A. Krosta, and B. Macke, Rev. Sci. Instrum. **49**, 526 (1978).
[21] C. H. Townes and A. L. Schawlow, *Microwave Spectroscopy*, (McGraw-Hill, New York, 1955), Chap. 10.
[22] A. Di Lieto, P. Minguzzi, and M. Tonelli, Phys. Rev. A **33**, 2109 (1986).
[23] R. L. Legan, J. A. Roberts, E. A. Rinehart, and C. C. Lin, J. Chem. Phys. **43**, 4337 (1965).
[24] P. Minguzzi and A. Di Lieto, J. Mol. Spectrosc. **109**, 388 (1985).
[25] G. Birnbaum, E. R. Cohen, and J. R. Rusk, J. Chem. Phys. **49**, 5150 (1968).